PLOS NEGLECTED TROPICAL DISEASES

RESEARCH ARTICLE

Identification of clinically approved small molecules that inhibit growth and affect transcript levels of developmentally regulated genes in the African trypanosome

Madison Elle Walsh[1], Eleanor Mary Naudzius[1], Savanah Jessica Diaz[1], Theodore William Wismar[1], Mikhail Martchenko Shilman[2], Danae Schulz[1]*

1 Department of Biology, Harvey Mudd College, Claremont, California, United States of America, **2** School of Applied Life Sciences, Keck Graduate Institute, Claremont, California, United States of America

* dschulz@g.hmc.edu

Citation: Walsh ME, Naudzius EM, Diaz SJ, Wismar TW, Martchenko Shilman M, Schulz D (2020) Identification of clinically approved small molecules that inhibit growth and affect transcript levels of developmentally regulated genes in the African trypanosome. PLoS Negl Trop Dis 14(3): e0007790. https://doi.org/10.1371/journal.pntd.0007790

Editor: Jayne Raper, Hunter College, CUNY, UNITED STATES

Received: September 12, 2019

Accepted: January 21, 2020

Published: March 13, 2020

Data Availability Statement: All relevant data are within the manuscript and its Supporting Information files.

Funding: The author received no specific funding for this work.

Competing interests: The authors have declared that no competing interests exist.

Abstract

Trypanosoma brucei are unicellular parasites endemic to Sub-Saharan Africa that cause fatal disease in humans and animals. Infection with these parasites is caused by the bite of the tsetse fly vector, and parasites living extracellularly in the blood of infected animals evade the host immune system through antigenic variation. Existing drugs for Human and Animal African Trypanosomiasis are difficult to administer and can have serious side effects. Resistance to some drugs is also increasing, creating an urgent need for alternative trypanosomiasis therapeutics. We screened a library of 1,585 U.S. or foreign-approved drugs and identified 154 compounds that inhibit trypanosome growth. As all of these compounds have already undergone testing for human toxicity, they represent good candidates for repurposing as trypanosome therapeutics. In addition to identifying drugs that inhibit trypanosome growth, we wished to identify small molecules that can induce bloodstream form parasites to differentiate into forms adapted for the insect vector. These insect stage parasites lack the immune evasion mechanisms prevalent in bloodstream forms, making them vulnerable to the host immune system. To identify drugs that increase transcript levels of an invariant, insect-stage specific surface protein called procyclin, we engineered bloodstream reporter parasites that express Green Fluorescent Protein (GFP) following induction or stabilization of the procyclin transcript. Using these bloodstream reporter strains in combination with automated flow cytometry, we identified eflornithine, spironolactone, and phenothiazine as small molecules that increase abundance of procyclin transcript. Both eflornithine and spironolactone also affect transcript levels for a subset of differentiation associated genes. While we failed to identify compounds that increase levels of procyclin protein on the cell surface, this study is proof of principle that these fluorescent reporter parasites represent a useful tool for future small molecule or genetic screens aimed at identifying molecules or processes that initiate remodeling of the parasite surface during life cycle stage transitions.

Author summary

African trypanosomes are unicellular parasites that infect humans and animals, causing a fatal disease known as sleeping sickness in humans and nagana in cattle. These diseases impose a severe economic burden for people living in Sub-Saharan Africa, where parasites are transmitted to humans and animals through the bite of the tsetse fly. Parasites living outside cells in humans and animals are attacked by the antibodies of the host immune system, but they can evade this attack by varying the proteins on their cell surface. In contrast, because flies do not have an antibody-mediated immune response, parasites living in flies do not vary the proteins on their cell surface. In this study, we performed a small molecule screen to identify compounds that either inhibit parasite growth or that affect transcript levels of genes associated with the transition to the insect stage. Parasites that are more similar to the insect-stage would be expected to be vulnerable to the mammalian immune system. We found 3 compounds that increased RNA levels for a gene that codes for an insect-stage surface protein. We also identified 154 compounds that inhibit parasite growth, and we hope these compounds might have potential as novel trypanosomiasis therapeutics.

Introduction

Trypanosoma brucei is a unicellular protozoan parasite that causes both Human and Animal African Trypanosomiasis (HAT and AAT, also known as sleeping sickness in humans and nagana in livestock, respectively). These diseases affect both humans and ungulates, causing a severe human and economic burden in regions of Sub-Saharan Africa where they are endemic [1]. Because trypanosomiasis primarily affects the rural poor, there is a paucity of efficacious drugs available. Moreover, all drugs in current use have severe side effects, some drugs used to treat late stage trypanosomiasis are highly toxic, and resistance to existing drugs is rising [2]. Thus, new strategies to treat trypanosomiasis are urgently needed.

We reasoned that existing clinically approved drugs might represent good candidates for alternate trypanosomiasis therapeutics, as they do not have to go through the same rigorous toxicity screening as newly developed drugs. With that in mind, we performed a small molecule flow cytometry-based screen using the Johns Hopkins University Clinical Compound Library and identified 154 small molecules that inhibit parasite growth, many of which have not previously been reported. We verified that several of the compounds from our screen inhibit growth with IC_{50}s in the low micromolar range. We hope that identification of these compounds will be a resource for researchers interested in repurposing existing compounds for treatment of neglected disease.

At the same time, we wondered whether we might be able to simultaneously screen for compounds that make trypanosomes poorly adapted to living in the bloodstream of their mammalian host. Specifically, identifying compounds that make the bloodstream parasite vulnerable to the host immune system could produce alternative trypanosomiasis therapeutics. Trypanosomes live extracellularly within the mammalian host and untreated infections are almost invariably fatal. This is because *T. brucei* has evolved a number of mechanisms that are effective at evading the mammalian host antibody response. Many of these depend on the expression and recycling of the Variant Surface Glycoprotein (VSG) coat that densely covers the surface of bloodstream trypanosomes [3]. There are thousands of antigenically distinct genetic variants of *VSG* in the genome [4], and by periodically switching the variant expressed on the parasite surface, the host antibody response can be effectively thwarted. This immune

evasion allows the parasite to live long enough within the mammalian bloodstream to be transferred to the tsetse fly insect vector following a bloodmeal, where it transitions to the insect-specific procyclic form. The environment of the fly is quite different from that of the mammalian bloodstream, and the parasite adapts itself accordingly by changing its morphology and metabolism [5]. Indeed, it has been shown that thousands of genes show altered transcript levels between bloodstream and procyclic forms [6–8]. A key event marking the transition from bloodstream to procyclic forms is the remodeling of parasite surface proteins to replace VSG with an invariant surface protein called procyclin, of which there are only four isoforms [9].

If bloodstream parasites were induced to express this invariant procyclin protein on the surface with a small molecule compound, this could provide a 'handle' for the mammalian immune system to eliminate parasites whose surface is usually a moving target due to the ever-shifting repertoire of VSGs. As an example, we previously showed that the small molecule bromodomain inhibitor I-BET151 has this effect in bloodstream form cells, resulting in the expression of procyclin on the surface and decreased virulence in a mouse model of infection [10]. In addition, others have attempted to identify compounds that induce expression of procyclin in bloodstream parasites using a GUS reporter assay [11,12].

To identify these compounds, we developed a fluorescent reporter system to allow us to easily detect transcript levels of the gene *EP1*, which codes for one isoform of the invariant insect-stage specific procyclin protein. Here we present proof of principle that our *EP1* fluorescent reporter can be used for flow cytometry-based screening using an autosampler. This allows for automated 96 well plate sampling without the need for a human operator, resulting in less labor-intensive flow cytometry-based drug library screens that can simultaneously screen for growth inhibition and a fluorescence-based phenotype. First, we showed that fluorescence levels in the reporter line faithfully mimic expected levels of *EP1* transcript in bloodstream, procyclic, and differentiating parasites. Second, we identified several compounds that increase *EP1* transcript levels in bloodstream form parasites.

While none of the compounds that increase *EP1* transcript levels are ideal as trypanosomiasis therapeutics, we think our reporter system holds promise both as a screening tool for other small molecule libraries and as a system to learn more about unidentified factors that stabilize procyclin protein after initiation of differentiation. Much progress has been made in elucidating the quorum sensing signaling pathways that are necessary to trigger parasite differentiation from the bloodstream form to the insect form via the stumpy intermediate [13–15]. It is also clear that RNA Binding Proteins (RBPs) play an important role in maintaining life cycle stage-specific mRNA levels and triggering differentiation events [16–19]. However, the gene regulatory mechanisms by which VSG transcription is halted and procyclin transcription is initiated and/or stabilized remain poorly characterized. Our long-term goal is to take advantage of this reporter system to perform genetic screens, allowing us to identify the key players responsible for stabilizing procyclin transcripts during differentiation from the bloodstream form to the procyclic form. This will allow us to unravel the missing link between environmental signals for differentiation that are received and transduced at the parasite surface and the downstream effect on transcript levels that ultimately allow the parasite to adapt from the bloodstream environment to the insect environment.

Methods

Culture growth and strain details

We used the Lister 427 L224 strain of bloodstream *T. brucei* parasites with a dual BES marked line that expresses *VSG3* from BES7 (with Neo^R downstream of the promoter) and a $Puro^R$ gene downstream of the BES1 promoter (expressing *VSG2*) [20]. Bloodstream parasites were

cultured in HMI-9 at 37˚C with 5% CO_2. Procyclic PF427 parasites were grown at 27˚C in SDM79.

Generation of the EP1/GFP reporter plasmid

DNA encoding GFP flanked by 314 bp immediately upstream of the *EP1* ORF and 279 bp immediately downstream of the *EP1* ORF was synthesized by Life Technology. Both upstream and downstream *EP1* fragments contain the entire 5' and 3' UTRs of *EP1*. The *5'UTR/GFP/3'UTR* fragment was amplified with PvuII and HindIII sites and cloned into the pyrFEKO $Hygro^R$ plasmid using the same sites. We then amplified a 289 bp homology region downstream of the *EP1* 3'UTR fragment with SpeI and XhoI, which was cloned downstream of the $Hygro^R$ gene using the same sites. The *5'UTR/GFP/3'UTR* fusion fragment was amplified using Forward ggccatcagctgagtcaatagtgcattttg and Reverse ggccataagcttgaatgaaaaaaaatagaagtgaaa primers. The downstream homology region was amplified using Forward ggccatactagtctttgaatttggatcttaaaattattattg and Reverse ggccatctcgagcaacttcagctgcggggc primers. For transfection into our Hygro resistant procyclic strain, the construct was modified to replace the $Hygro^R$ gene with a $Puro^R$ gene.

Strain construction

Transfection of bloodstream form parasites was performed using an AMAXA Nucleofector. Parasites were resuspended in 100μl T cell solution with 10μg linearized DNA and electroporated on the X001 setting. Following transfection, cells were grown in 5μg/ml Hygromycin (Invivogen). PF cells were transfected using the same procedure, but following transfection the cells were plated into conditioned media in 0.1μg/ml Puromycin (Invivogen). Correct integration of the construct in transfected cells was tested using PCR with a forward primer upstream of the 5'UTR of *EP1* (gtccgataggtatctcttattagtatag) and a reverse primer within the *GFP* gene (agaagtcgtgctgcttcatgtggt). Successful isolation of genomic DNA was confirmed using control primers that amplify the downstream *EP1* homology region: For ggccatactagtctttgaatttggatcttaaaattattattg and Rev ggccatctcgagcaacttcagctgcggggc.

Differentiation

Bloodstream parasites were spun down and resuspended in differentiation media [21] supplemented with 6 mM cis-aconitate (Sigma-Aldrich A3412) at 27˚C for three days.

Sytox Orange staining

Cells were resuspended in 5μM Sytox Orange (Fisher Scientific S11368) and incubated for 15 minutes at 37˚C prior to flow cytometric analysis.

Flow cytometry

All flow cytometry was done with a Novocyte 2000R from Acea biosciences. Procyclin or VSG protein expression was measured following three to five days of drug treatment at 33 μM, after which parasites were stained for 10 minutes on ice with anti-EP1 (Cedarlane CLP001A) antibody or anti-VSG224 antibody. Cells were washed twice in HMI9 prior to analysis.

Western blotting

8 million parasites were pelleted, resuspended in 2X Laemmli Sample Buffer and boiled at 95˚C for 5 minutes. Proteins from this whole cell extract were separated by SDS-PAGE on a 4–20% gradient gel and transferred to PVDF membrane. Blocking was performed in 5% milk in PBS for 1 hour. Membranes were incubated with anti-procyclin antibody (Cedarlane

CLP001AP) or anti-H3 (a generous gift from Christian Janzen) in 5% milk in PBS. After washing in TBS supplemented with 0.1% Tween-20, membranes were incubated with goat anti-mouse or goat anti-rabbit secondary antibody (IRDye 800 CW from Biorad) and imaged on a Licor instrument.

Data analysis and statistical tests

Drug screen. A total of 1,585 drugs were tested from the Johns Hopkins University Clinical Compound Library, which had patented compounds removed prior to drug screening. Drug screening was conducted with the *EP1/GFP* parasites plated with 1,000 cells in 100 μL cultures and 33 μM of drug. After 3 days of growth, cells were screened for GFP fluorescence via flow cytometry. To test for autofluorescence of candidate hits, 300,000 cells/100μL culture were plated with 33 μM of each drug and immediately screened for fluorescence via flow cytometry. Each plate also contained three wells of negative control cells treated with DMSO and a well of positive control cells treated with 20μM I-BET151 (Sigma-Aldrich).

All samples with an average median GFP fluorescence intensity that was 1.5-fold or higher than the +DMSO control from the first two rounds of screening were selected for further screening. Drugs tested in triplicate were subjected to a two-sided, unpaired Student's t-test. To identify drugs that inhibit trypanosome growth or those that are trypanocidal, we used flow cytometry to calculate total cell counts/10μl of volume. Control cells typically showed ~35000 cells/10μl volume within the live gate, so we identified trypanocidal drugs as those that resulted in counts between 350–3500, 35–350, and <35 in the live gate.

Confirmation of drug hits. 1 mL cultures of *EP1/GFP* reporter cells were treated with 33 μM of eflornithine (Sigma-Aldrich 1234249), phenothiazine (Sigma-Aldrich P14831), spironolactone (Sigma-Aldrich S3378), or vehicle control and grown for three days. The cells were then screened for GFP fluorescence via flow cytometry.

Growth curves. 1 mL cultures of *EP1/GFP* reporter cells were plated at 100,000 cells/ml and treated with 33 μM of eflornithine (Sigma-Aldrich 1234249), phenothiazine (Sigma-Aldrich P14831), spironolactone (Sigma-Aldrich S3378), or vehicle control and counted daily by hemocytometer. Each day following counting, cells were diluted back to 100,000 cells/ml. For growth curve analysis by flow cytometry, 200 μl cultures of parasites were plated at 100,000 cells/ml and treated with 33 μM of phenothiazine (Sigma-Aldrich P14831), triprolidine hydrochloride (Sigma-Aldrich T6764), flunarizine hydrochloride (Sigma-Aldrich F8257), aprepitant (Sigma-Aldrich SML2215), bufexamac (Sigma-Aldrich B0760), clemastine fumarate salt (Sigma-Aldrich SML0445) or vehicle control. Parasites were stained daily with Sytox Orange and a fixed volume of cells was analyzed by flow cytometry. The number of live cells was calculated as the number of Sytox Orange negative cells falling within the live gate. Each day following flow analysis, cells were diluted back to 100,000 cells/ml according to the number of live cells counted.

IC_{50} analysis. 2,000 parasites were plated in a 200μl volume of HMI9 (10,000 cells/ml) at the indicated concentrations of each drug and grown for 48 hours at 37˚C with 5% CO_2. Parasites were then stained with Sytox Orange and the number of Sytox Orange negative parasites falling within the live gate was calculated using flow cytometry with a fixed volume of cells. Data were analyzed and fitted using GRMetric, an R package for calculation of dose response metrics based on growth rate inhibition [22]. Growth rate values are calculated individually for each treatment using the formula

$$GR = 2\hat{}(\log_2(\text{cellcount}/\text{cellcount\_control})/\log_2(\text{cellcount\_control}/\text{cellcount\_time}_0) - 1$$

The data are fitted with a sigmoidal curve

$$GR(c) = GR_{inf} + (1-GR_{inf})/(1 + (c/(GEC_{50}))\hat{}Hill)$$

where GR_{inf} = GR(count>inf), reflecting asymptotic drug efficacy. GEC_{50}, the drug concentration at half-maximal effect, Hill, the Hill coefficient of the fitted GR curve reflecting how steep the dose-response curve is.

Cell cycle analysis. Cells were fixed using 1% formaldehyde in PBS for 5 minutes. Cells were then washed three times in PBS and then resuspended in a solution of 0.2 mg/ml RNAse and 0.05 mg/ml propidium iodide in PBS. Following a 2-hour incubation at 37˚C, cells were analyzed by flow cytometry.

Quantitative PCR analysis. For quantitative PCR to quantify mRNA levels, RNA was extracted from parasites treated with drug or vehicle control for 3 days using RNA Stat-60 (Tel-Test) following the manufacturer's protocol and quantified on a NanoDrop2000c. 2.5μg of RNA was used to generate cDNA using the SuperScript IV VILO Master Mix (Fisher Scientific 11756050) according to the manufacturer's protocol. cDNA was amplified using 2X Sybr green master mix (Life Technologies 4309155) and primers and quantified on an Eppendorf Realplex2 instrument. Primers used were as follows: *Tb427.10.10260 EP1*, tctgctc gctattcttctgttc, cctttgcctcccttagtaagac, *Tb927.6.510 GPEET* agtcggctagcaacgttatc, ttctggtccggt ctcttct, *Tb927.9.11600*, *GIM5B*, ttgcgaggatgggtgatg, gggtttggagagggaagttaat, *Tb927.10.2010*, *HK1*, gtcagcacttactcccatcaa, acgacgcatcgtcaatatcc, *Tb927.10.5620*, *ALD*, gtctgaagctgttgttcgtttc, cacctcaggctccacaatag, *Tb927.10.10220*, *PAG2*, aggagatacgaggaatgagaca, tcttcaaacgcccggtaag, *Tb927.10.14140 PYK1*, gagaaggttggcacaaagga, tcacaccgtcgtcaacataaa, *GFP*, ctacaacagccacaagg tctat, ggtgttctgctggtagtg, *Tb927.10.9400*, *SF1*, ggtatggttcatcaggagttgg, cgttagcactggtatccttcag.

Mammalian cell growth assay. RAW264.7 mouse macrophage or C32 human melanoma cells were maintained in DMEM (Sigma-Aldrich) supplemented with 10% fetal bovine serum, as well as 100 μg/mL penicillin and 100 μg/mL streptomycin. 10,000 RAW264.7 cells per well were seeded in 96-well plates in 100 μl/well 24 hours before the assay. On the day of the assay, 0.75 or 1.5 μl of 3.3 mM JHCCL drugs were added to 150 μl of cell-containing media to achieve 16 or 33 μM of each compound per well, respectively. Cells were treated with drugs for 6 hours at 37 ˚C and 5% CO_2. C32 cells were treated with drugs for 24 hours. Determination of cell viability by 3-(4,5-dimethylthiazol-2-yl)-2,5-diphenyltetrazolium bromide (MTT) assay was performed as described [23]. Cell viability is shown as the percentage of surviving cells obtained relative to cells treated with DMSO as vehicle control (100%).

Accession numbers.

EP1, Tb927.10.10260
PAG2, Tb927.10.10220
GPEET, Tb927.6.510
HK1, Tb927.10.2010
GIM5B, Tb927.9.11600
ALD, Tb927.10.5620
PYK1, Tb927.10.14140
SF1, Tb927.10.9400

Results

Identification of *in vitro* inhibitors for *T. brucei* growth

To identify existing compounds that might be repurposed as trypanosomiasis therapeutics, we obtained the Johns Hopkins University Clinical Compound Library of 1,585 small molecule drugs. 1082 of these compounds are FDA approved while the remaining are foreign approved

drugs. We plated 1000 bloodstream parasites in 100μl of media in a 96 well plate format. We then added 1μl of each drug to the well for a final concentration of 33μM. We chose this concentration because it had been used previously with this same library to successfully identify compounds that cross-inhibit pathogenic agents and the host proteins they exploit [24]. We reasoned that follow-up experiments could be used to determine whether specific compounds could still inhibit growth in a more desirable nM or low μM range. Because our screen used a flow cytometer that can be programmed to analyze a fixed volume of cells, we were easily able to identify drugs that slowed trypanosome growth after 3 days of treatment by simply counting the number of analyzed cells that fell within a live cell gate. The entire assay was performed in duplicate for each drug in the library. We binned each drug into four categories: highly inhibitory, inhibitory, slightly inhibitory, and not inhibitory (Table 1). Our DMSO vehicle treated cells averaged roughly 35,000 cells in the live gate at the end of the treatment. 35 drugs were classified as highly Inhibitory because they resulted in 35 cells or less in the live gate. 102 drugs with 36–350 cells in the live gate were classified as Inhibitory, 17 drugs with 351–3,500 live gate cells were classified as slightly inhibitory, and any samples with greater than 3500 cells were classified as not inhibitory (the remaining 1,431 samples, Table 1).

For the most highly inhibited category of drugs, we searched the literature to see if they had previously been characterized as anti-trypanosomal. Berberine, ipecac syrup, disulfiram, methylene blue hydrate, promethazine hydrochloride, perphenazine, promazine hydrochloride, and trifluprom azine have all previously been reported to inhibit growth in *T. brucei* and our results agree with those previously published reports [25–29] (S1 Table, S2 Table). Several other drugs, including nitrofurazone, aminacrine, clemastine fumarate, bepridil hydrochloride, amiodarone hydrochloride, prochlorperazine dimaleate, protriptyline hydrochloride, fluoxetine hydrochloride, apomorphine hydrochloride, and proadifen hydrochloride have been shown to inhibit growth in *T. cruzi* [27,30–38]. Finally, cyproheptadine hydrochloride was shown to inhibit growth in *T. evansi* (S1 Table) [39]. We also identified a number of drugs that inhibit *T. brucei* growth *in vitro* that, to our knowledge, have not previously been studied in this context (S1 Table), including antimalarials, antibacterials, antiseptics, anesthetics, antihypertensives, antiemetics, antidepressants, vitamins, and a vasodilator. In addition to these highly inhibitory drugs, a further 119 drugs were shown to have a 10–100 fold inhibitory effect on parasite growth, including homidium bromide (used to treat cattle [40]) and pentamidine, a well- established trypanosomiasis drug [41] (S3 Table, S4 Table).

We additionally compared the results from this study to two other recent NTD-focused drug screens. One of these used the Medicines for Malaria Venture Pathogen box dataset (https://www.mmv.org/mmv-open/pathogen-box/about-pathogen-box#composition_), which includes 70 anti-kinetoplastid compounds. We cross-referenced all 400 compounds in the NTD Pathogen box with the compounds in our library and found that five of the compounds that were identified as inhibiting growth in our study were also included in the Pathogen Box. These include three compounds that were used as reference compounds in the Pathogen Box data: the antimalarial drug primaquine, the antibacterial drug clofazimine, and the antiprotozoal drug pentamidine. Both primaquine and clofazimine have previously been reported

Table 1. Summary of drugs that cause growth inhibition or cell death.

Level of Inhibition	Number of Drugs
Highly Inhibitory (0–35 live cells)	35
Inhibitory (36–350 live cells)	102
Slightly Inhibitory (351–3500 live cells)	17
Not Inhibitory	1431

https://doi.org/10.1371/journal.pntd.0007790.t001

to be active against *T. cruzi* [42,43], while pentamidine is used against *T. brucei* infections. Similar to our study, fluoxetine was reported to be effective against kinetoplastids in the Pathogen Box data. Finally, clemastine fumarate was reported to be effective against trichuriasis caused by the human whipworm in the Pathogen Box data, but was not mentioned in the context of kinetoplastid infections. We further compared results from our study to a set of compounds found to be inhibitory to *T. brucei* growth in a recent screen from GSK (https://www.ebi.ac.uk/chembl/g/#browse/activities/filter/document_chembl_id%3ACHEMBL3430912); however, none of the compounds identified in this screen overlapped with the compounds in our library.

In addition to assaying these drugs for their effect on trypanosome growth, we also measured percent survival after treatment for 24h with 16μM drug for two different cell lines: murine Raw264.7 macrophages and human C32 melanoma lines (S2–S4 Tables). Additional toxicity information gathered from pubchem is provided in S5 Table. These additional data can be used to help prioritize the drugs with the highest mammalian cell line survival rate and the lowest toxicity. We hope that this list can be used as a resource for those in the trypanosomiasis drug development field.

Confirmation that drugs identified in the screen inhibit trypanosome growth

To confirm that the drugs identified in the screen did indeed inhibit parasite growth, we ordered fresh stocks of six drugs from Sigma-Aldrich and measured growth inhibition. We chose three drugs from our most highly inhibitory category: flunarizine hydrochloride, aprepitant, and clemastine fumarate. Clemastine fumarate is an antihistaminic drug that has been shown to inhibit growth in *T. cruzi* [31]. Aprepitant is an antiemetic and flunarizine hydrochloride is a vasodilator. To our knowledge neither of these latter two have been studied for their effects on kinetoplastids. In addition to these three highly inhibitory compounds, we chose one drug from our inhibitory category (triprolidine) and two drugs from our slightly inhibitory category (phenothiaizine and bufexamac). Neither triprolidine nor bufexamac have been shown to inhibit trypanosome growth, while phenothiazine has previously been shown to be strongly inhibitory [44,45]. To assess the effect of each of these six drugs on trypanosome growth, we adopted a flow cytometry assay using the nucleic acid stain Sytox Orange, which positively stains dying and dead cells with compromised membranes. Parasites were plated at 100,000 cells/ml, and an aliquot of parasites was stained with Sytox Orange after 24h of growth. A fixed volume of cells was then analyzed by flow cytometry and the number of live cells was determined by gating on Sytox Orange negative populations whose size (measured by forward scatter) is consistent with healthy parasites (Fig 1A). Whereas healthy cells do not stain positively with Sytox Orange (Fig 1A, left), those treated with an inhibitory drug do show populations of positively staining Sytox Orange parasites as well as populations of smaller particles that represent dead cells and debris (Fig 1A, right). Based on the number of cells in the live gate, the remaining unstained parasites were diluted back down to 100,000 parasites/ml. The growth curves in Fig 1B show that parasites treated with five of the six drugs we tested had a severe growth inhibited phenotype, while treatment with triprolidine had no appreciable effect on growth (S8 Table). Survival data for mammalian cell lines treated for 24h at 33μM for all verified growth inhibition drugs is provided in S6 Table.

We went on to estimate the IC_{50} values for each of the six drugs by growing parasites for 48h in a range of concentrations. Five of the six drugs showed IC_{50} values between 3.7 and 12.3μM (Fig 1C, see insets). Consistent with our observations on cell growth, the IC_{50} value measured for triprolidine was very high (S1 Fig inset) and the r^2 value for this drug indicates a

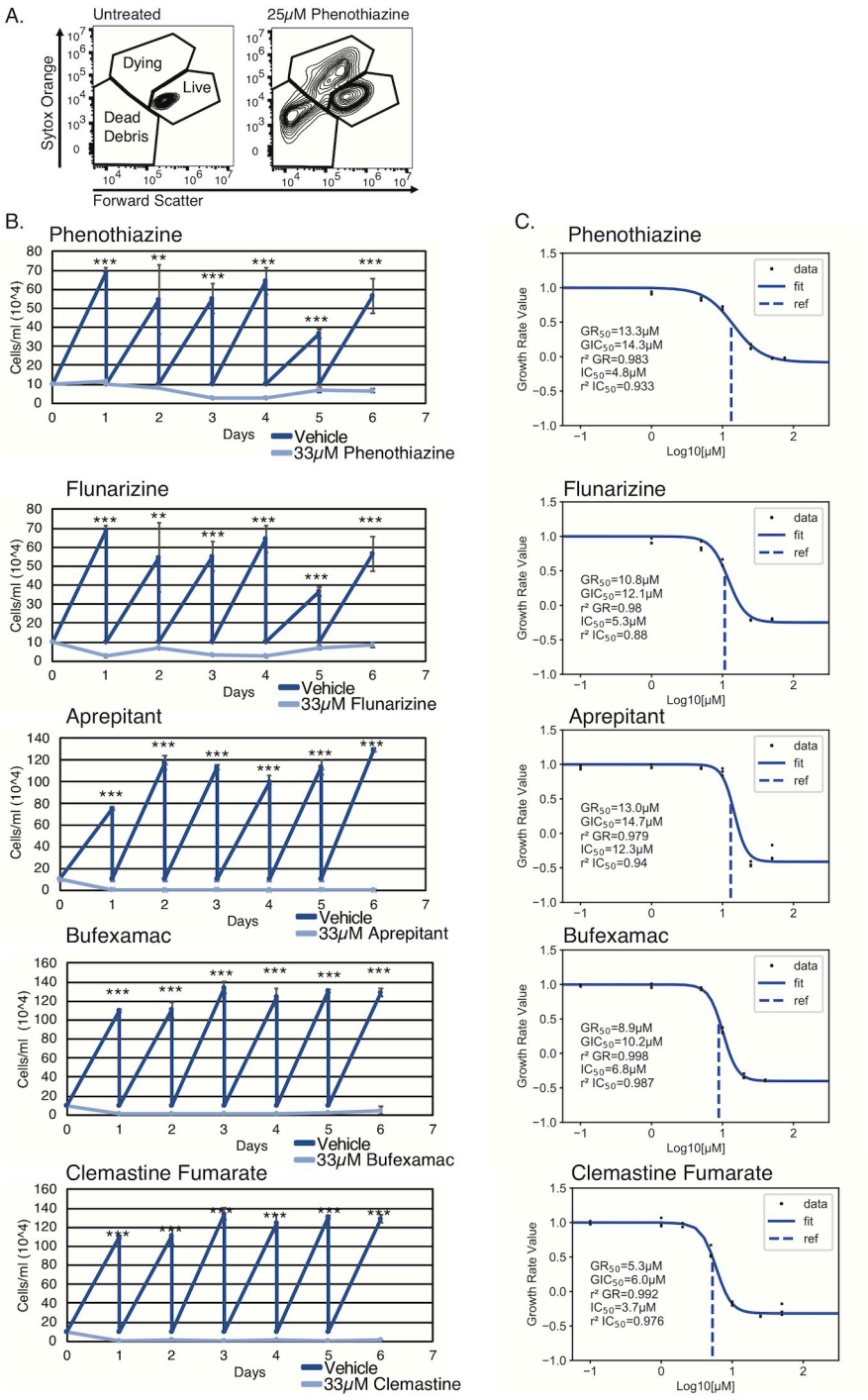

Fig 1. Confirmation of growth inhibition for a subset of drugs identified in the drug screen. (A) Flow cytometry plot showing forward scatter vs Sytox Orange staining to illustrate how live cells were gated. (Left) untreated parasites, (Right) parasites treated with 25μM phenothiazine. (B) Growth curves of parasites treated with the indicated drugs or vehicle control over a period of 6 days. Dark blue, vehicle control treated cells, Light blue, drug treated cells. Error bars indicate standard deviation of 3 biological replicates. *, **, *** indicates $p < 0.05$, $p < 0.01$, and $p < 0.001$ respectively as measured by an unpaired two-sided Student's T test. (C) Percent growth inhibition over a range of concentrations for the indicated drug. Data were fitted and indicated values calculated using the GRMetrics R package. GR_{50}, the concentration at which the effect reaches a growth rate (GR) value of 0.5 based on interpolation of the fitted curve (dashed lines). GIC_{50}, the drug concentration at half-maximal effect for calculated growth rate. r^2 GR, the coefficient of determination for how well the GR curve fits to the data points. IC_{50}, the concentration at which relative cell

count = 0.5. r^2 IC_{50}, the coefficient of determination for how well the traditional curve fits to the data points. See methods for more details.

https://doi.org/10.1371/journal.pntd.0007790.g001

relatively poor fit for the data. Therefore, it should be noted that the screen can produce some false positives, and promising candidates need to be verified with fresh stocks prior to further study. Interestingly, we did not observe consistently higher IC_{50} values for drugs in the slightly inhibitory (phenothiazine, bufexamac) category when compared to those in the highly inhibitory category (aprepitant, clemastine fumarate, flunarizine). We conclude that compounds with only a 15-25-fold reduction in cell counts as measured in our screen can still have highly inhibitory effects on growth.

Construction and validation of the *EP1/GFP* reporter cell line

We reasoned that a flow cytometric based screen could allow for simultaneous screening for compounds that inhibit trypanosome growth and for compounds that increase transcript levels of the invariant insect-stage specific procyclin gene *EP1*. In order to facilitate flow cytometric screening for compounds that increase transcript levels of the *EP1* gene in bloodstream parasites, we integrated a construct containing *GFP* flanked by native EP1 5' and 3' UTRs at the endogenous *EP1* locus (Fig 2A). It should be noted that an increase in GFP expression in parasites harboring this construct could be from higher levels of transcript being produced, increased stability of the transcript, or both. The construct was integrated in both bloodstream and procyclic parasites, and the second *EP1* allele was left intact. A PCR assay confirmed the correct integration of the reporter construct in both bloodstream and procyclic parasites (Fig 2A). We expect that if this reporter construct faithfully recapitulates native *EP1* expression, GFP levels should be relatively low in bloodstream form parasites and high in procyclic parasites. Fig 2B shows that GFP levels in *EP1/GFP* reporter cells are low in bloodstream parasites and high in procyclic parasites, as expected. We also expect that GFP expression in bloodstream *EP1/GFP* reporter parasites should increase when parasites are induced to differentiate to the procyclic form using cis-aconitate and incubation at 27˚C, and we found that this was indeed the case (Fig 2C). Finally, we tested the effect of the bromodomain inhibitor I-BET151, which was previously shown to induce *EP1* expression in bloodstream parasites [10]. Treatment of bloodstream *EP1/GFP* reporter cells with I-BET151 resulted in an increase in GFP expression after 3 days, and the effect was more pronounced after 5 days (Fig 2D). We conclude that *GFP* expression mirrors the expected expression of *EP1* in the *EP1/GFP* reporter line by all the metrics tested.

A proof of principle screen shows that the reporter strain can be used to identify small molecules that increase transcript abundance of the procyclin gene *EP1*

Our *EP1/GFP* reporter parasites were used for the flow cytometric screen of the Johns Hopkins University Clinical Compounds used to identify inhibitory compounds described above. After 3 days of growth, we subjected each well to analysis by flow cytometry to measure the number of parasites in the live gate and the level of *EP1/GFP* expression. Each plate also contained parasites growing in DMSO to serve as a solvent control and I-BET151-treated parasites as a positive control. This assay was performed in duplicate for each of the drugs. After the two initial assays, the median GFP fluorescence intensity was calculated for DMSO-treated parasites and drug treated parasites. Any drug that caused a 1.5-fold increase in average median GFP fluorescence intensity in drug-treated parasites compared to DMSO-treated control parasites was

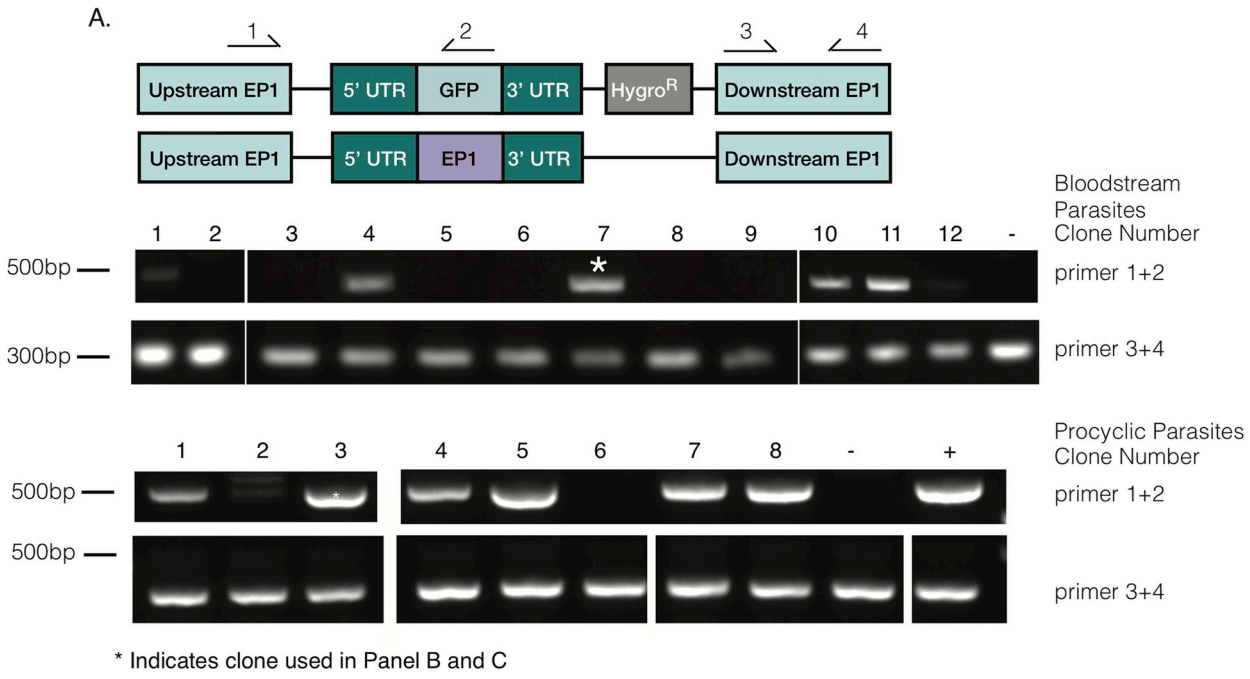
A.
1
2
3
4
Upstream EP1
5' UTR
GFP
3' UTR
Hygro^R
Downstream EP1
Upstream EP1
5' UTR
EP1
3' UTR
Downstream EP1
Bloodstream Parasites Clone Number
1 2 3 4 5 6 7 8 9 10 11 12 -
500bp
primer 1+2
300bp
primer 3+4
Procyclic Parasites Clone Number
1 2 3 4 5 6 7 8 - +
500bp
primer 1+2
500bp
primer 3+4
* Indicates clone used in Panel B and C

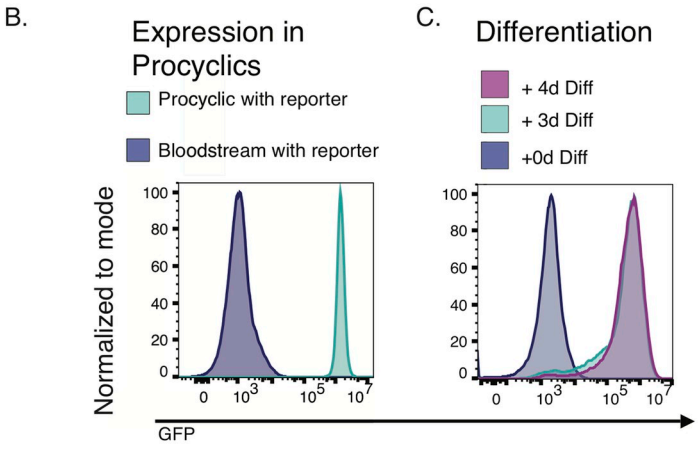
B.
Expression in Procyclics
Procyclic with reporter
Bloodstream with reporter
C.
Differentiation
+ 4d Diff
+ 3d Diff
+0d Diff
Normalized to mode
GFP

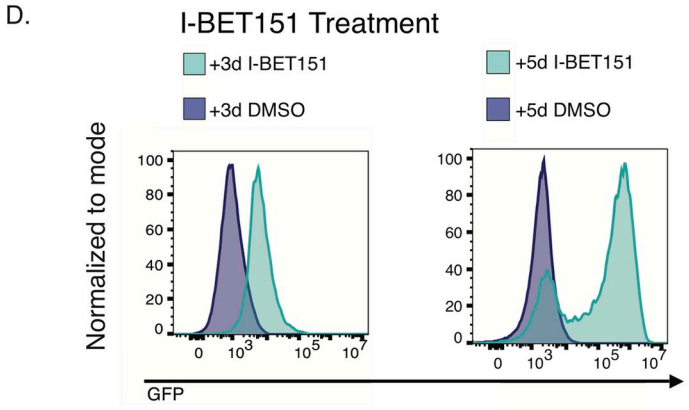
D.
I-BET151 Treatment
+3d I-BET151
+3d DMSO
+5d I-BET151
+5d DMSO
Normalized to mode
GFP

Fig 2. Validation of the *EP1/GFP* reporter construct. (A) (Top) Schematic showing the endogenous *EP1* locus following replacement of one allele with the *EP1/GFP* construct, wherein *GFP* is flanked by the native *EP1* 5' and 3' UTRs and marked with a Hygromycin resistance gene. The second *EP1* allele remains intact. Arrows indicate primers used to screen clones for correct integration of the reporter. Primers 1 and 2 were used to confirm integration, and primers 3 and 4 were used as a control for the presence of genomic DNA. Diagram shown is not to scale. (Middle) Gel electrophoresis of PCR products generated from 12 clones of bloodstream form parasites transfected with the *EP1/GFP* reporter construct. The parental line was used as a negative control (-). 4 clones showed correct integration by this assay, and (*) indicates the clone that was used for subsequent screening. Numbers on the right-hand side of the gel indicate the primer pair used. (Bottom) Same as the middle panel but for procyclic parasites transfected with the *EP1/GFP* reporter construct. The parental line was used as a negative control (-) and genomic DNA from a positively scoring bloodstream clone was used as a positive control (+). 6 clones scored positive and (*) indicates the clone used for flow cytometry in the panel below. (B) Flow cytometry plot for *GFP* expression in bloodstream and procyclic *EP1/GFP* reporter parasite clones. (C) Flow cytometry plot showing *GFP* expression in uninduced bloodstream *EP1/GFP* reporter parasites and in these same parasites induced to differentiate to procyclic forms using 6mM cis-aconitate and incubation at 27˚C. (D) Flow cytometry plot showing *GFP* expression in bloodstream *EP1/GFP* parasites treated with the bromodomain inhibitor I-BET151 or vehicle control for 3 days (left) or 5 days (right).

https://doi.org/10.1371/journal.pntd.0007790.g002

moved forward to the third round of screening. During this third round, in addition to the 3-day assay, drug-treated parasites were immediately subjected to analysis by flow cytometry following the addition of the drug to eliminate any drugs that were themselves fluorescent. After this third round, the median GFP fluorescence intensities for drug-treated parasites and solvent control-treated parasites were calculated again, and a Student's t-test was performed to identify drugs that caused a significant increase in median GFP fluorescence intensity. For those drugs that induced a significant shift, we imposed a 2-fold median GFP fluorescence intensity cutoff (S7 Table). This left us with 9 candidate drugs, for which we ordered fresh stocks from Sigma-Aldrich. Parasites were again subjected to the 3-day flow cytometry assay, except this time they were grown in 1ml cultures. We were able to replicate the increase in *EP1/GFP* expression for Spirinolactone, Phenothiazine, and Eflornithine (Fig 3). Notably, all of our false positives for *EP1/GFP* expression inhibited cell growth (S7 Table). We hypothesize that the low cell counts produced noise in the data and that dying cells may have produced autofluorescence in the GFP channel. During follow-up experiments, the higher number of cells assayed by flow cytometry may have alleviated one or both of these problems.

Of the drugs we identified as increasing *EP1/GFP* expression, eflornithine treated bloodstream parasites have previously been reported to show some similarities to stumpy cells, although these stumpy-like forms are not competent to differentiate to procyclic forms [46]. As stumpy forms have been shown to transcriptionally preadapt themselves to insect stage procyclic cells by upregulating procyclic specific transcripts [47], the increase in *EP1/GFP* expression in eflornithine treated parasites is consistent with these parasites sharing some characteristics of stumpy form parasites. As mentioned above, phenothiazine and its derivatives have previously been reported as anti-protozoal, strongly inhibiting cell growth in *T. brucei* [44,45]. Lastly, to our knowledge, spironolactone has not been studied in the context of *T. brucei* infection, although it has been tested for its effects on myocardial protection in a model of Chagas disease [48]. Spironolactone is used for the treatment of hirsutism, as is eflornithine, which is one of the most important anti-trypanosomal drugs in current use [49].

Phenothiazine causes severe growth defects and cell cycle abnormalities

We wished to determine if the observed increase in *EP1/GFP* expression for each candidate drug was a non-specific result of cell cycle arrest, so we tested the drugs that caused a measurable increase in *EP1/GFP* expression for their effect on parasite growth. While neither spironolactone nor eflornithine induced a profound effect on parasite growth at 33μM, phenothiazine caused a growth arrest in treated cells by 24h (Fig 4A). As expected, eflornithine did have effects on parasite growth at higher concentrations of 120μM (Fig 4A). To test the effect of each of these drugs on cell cycle, we performed propidium iodide staining and flow cytometry on parasites treated with each of the drugs for three days. In keeping with our observations of

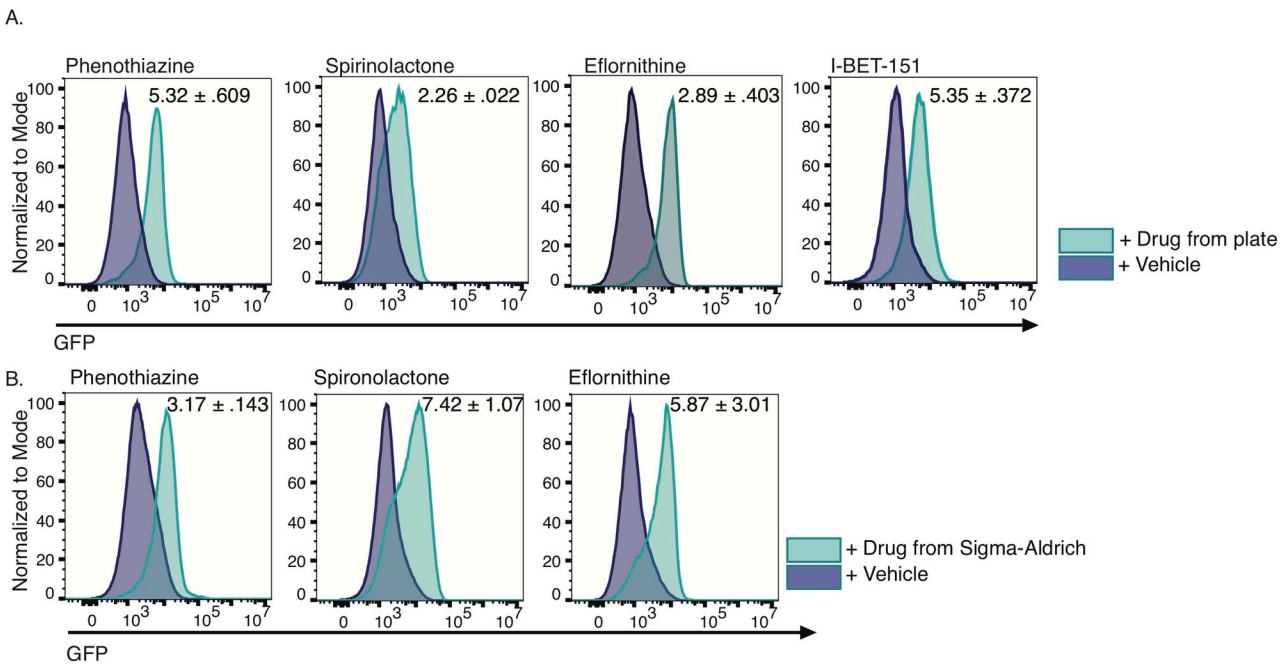

Fig 3. Three drugs from the small molecule library produced a reproducible shift in *EP1/GFP* expression. (A) Flow cytometry plots of *GFP* expression in *EP1/GFP* reporter parasites grown for 3 days in the presence of 33μM drug sourced from library plates or vehicle control. Inset indicates average fold change in median fluorescence intensity with standard deviation from 3 replicates of the experiment. (B) Flow cytometry plots of *GFP* expression in *EP1/GFP* reporter parasites grown for 3 days in the presence of fresh drug at 33μM sourced from Sigma-Aldrich. Inset indicates average fold change in median fluorescence intensity with standard deviation from 3 replicates of the experiment.

https://doi.org/10.1371/journal.pntd.0007790.g003

cell growth, phenothiazine treated parasites exhibited severe cell cycle abnormalities after 3 days of treatment (Fig 4B). We further tested phenothiazine treatment of parasites at earlier time points and found significant cell cycle abnormalities within 24h of treatment (Fig 4C). At 1 day the most pronounced effects were the accumulation of parasites in the G2 phase of the cell cycle, a decrease in S phase cells, and the appearance of multinucleated cells. At 2 days an accumulation of parasites lacking a nucleus (zoids) was apparent, and this effect was even more pronounced at 3 days (Fig 4D). The percent of parasites in each of the cell cycle stages was significantly different at all time points tested when compared to the DMSO treated controls. These results are in keeping with previously published reports that show that phenothiazine treated parasites exhibit severe growth defects through inhibition of trypanothione reductase [44,50]. We conjecture that the effect of phenothiazine on *EP1/GFP* expression might be a non-specific stress response, while this does not appear to be the case for either spironolactone or eflornithine. Survival data for mammalian cell lines treated for 24h at 33μM for all verified *EP1/GFP* drugs is provided in S6 Table.

Surface protein expression of procyclin is not observed following treatment with drugs observed to increase *EP1/GFP* transcript levels

We tested whether the increase in *EP1/GFP* transcript levels corresponded to an increase in the corresponding procyclin protein on the parasite surface. Because our antibody to procyclin fluoresces in the same channel as GFP, we treated the parental strain for our reporter strain for 5 days with 33μM eflornithine, phenothiazine, and spironolactone, stained the parasites with anti-procyclin, and assayed procyclin protein expression by flow cytometry. I-BET151 was used as a positive control as it has previously been shown to increase surface protein

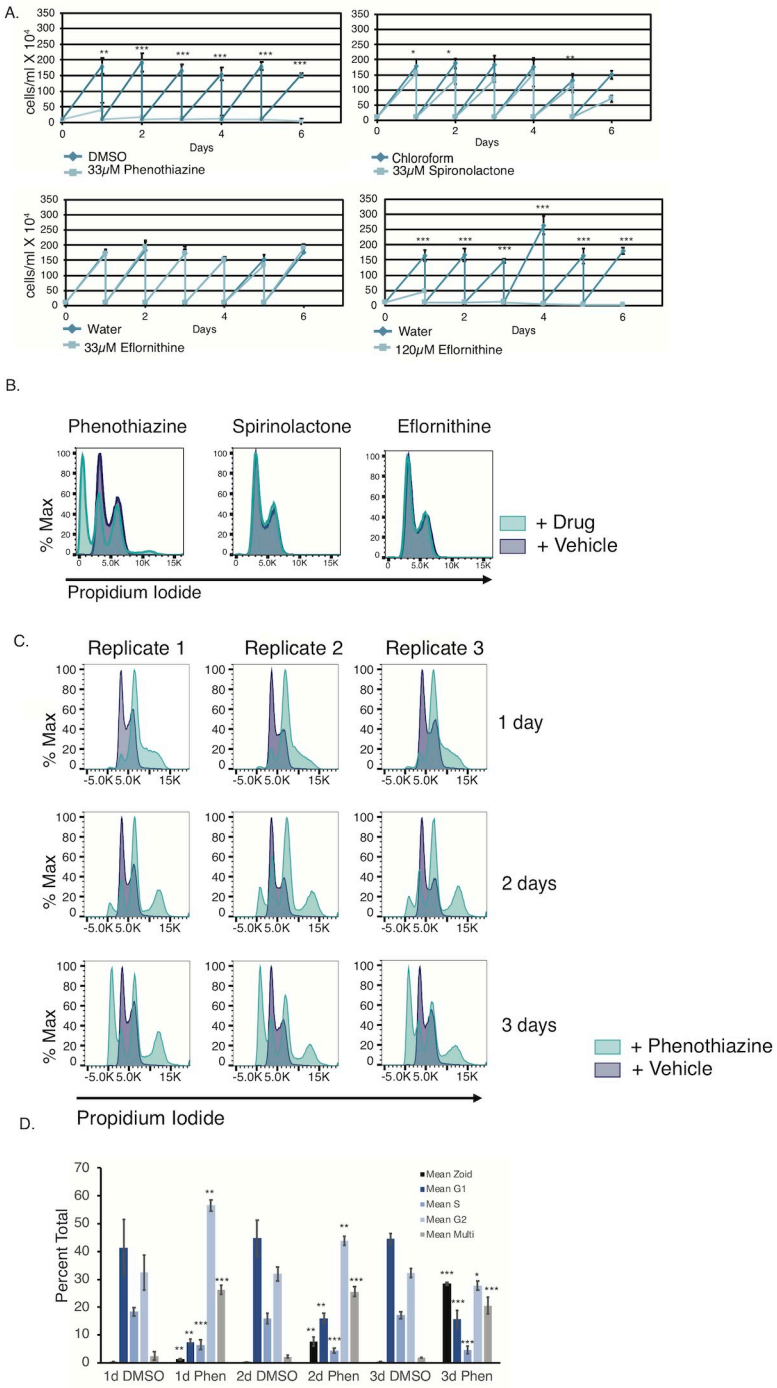

Fig 4. Phenothiazine-treated parasites are growth-arrested and show cell cycle defects. (A) Growth curves of bloodstream parasites grown in the presence of the indicated drug or vehicle control for 6 days. Parasites were counted daily on a hemacytometer and diluted to 100,000 cells/ml after counting. Error bars indicate standard deviation of 3 biological replicates. *, **, *** indicates $p < 0.05$, $p < 0.01$, and $p < 0.001$ respectively as measured by an unpaired two-sided Student's t-test. (B) Flow cytometry plot using propidium iodide staining to assay cell cycle in bloodstream parasites treated with the 33μM of the indicated drug or vehicle control for 3 days. (C) Flow cytometry plot using propidium iodide staining to assay cell cycle in bloodstream parasites treated with the 33μM phenothiazine or vehicle control for the indicated number of days. (D) Quantification of the data collected in (C) showing the percent of cells in each phase of the cell cycle. *, **, *** indicates $p < 0.05$, $p < 0.01$, and $p < 0.001$ respectively as measured by an unpaired two-sided Student's t-test.

https://doi.org/10.1371/journal.pntd.0007790.g004

expression of procyclin [10]. Previous experiments showed that the highest level of procyclin expression for I-BET151 was at 5 days, so we used a similar treatment for our new drug candidates and replenished the drug every two days. None of the drugs produced measurable procyclin protein on the parasite surface after treatment (Fig 5A), and we could not detect procyclin protein in whole cell lysates of drug-treated parasites by western blot (S2 Fig). An increase in *EP1* transcript abundance without a concomitant increase in protein expression has been observed before in the context of DNA replication mutants [51]. While eflornithine is already in use as a trypanosome therapeutic and phenothiazine may have potential as a therapeutic based on its effect on cell growth, we conclude that spironolactone is not a promising drug candidate for trypanosomiasis since the effect on *EP1* transcript levels is not recapitulated at the level of protein (Fig 5A). However, future studies beyond the scope of this work might aim to identify the protein target of spironolactone to try and ascertain whether this protein maintains low levels of *EP1* transcript in bloodstream cells.

A previous study seeking to identify compounds that increase *EP1* transcript levels reported that a number of compounds that increased *EP1* transcript levels also had an effect on the level of VSG protein on the surface, as measured by flow cytometry [11,12]. The general effect observed was an increase in VSG median fluorescence intensity (MFI), and the authors speculated that this was due to loss of the VSG coat from the surface, which resulted in more epitopes exposed for antibody binding [12]. Our group also reported an increase in VSG MFI prior to complete loss of VSG protein from the surface following treatment with the bromodomain inhibitor I-BET151 [10]. Therefore, we performed flow cytometry using anti-VSG antibodies on parasites treated for 2 or 3 days with phenothiazine, spironolactone, and eflornithine. No effect on MFI for VSG was detected for spironolactone or eflornithine, indicating that an increase in *EP1/GFP* transcript levels is not sufficient to alter the VSG MFI (Fig 5B). Both 2 and 3 days of phenothiazine treatment produced one population of parasites with higher VSG MFI compared to DMSO-treated controls and a second population of phenothiazine-treated parasites with lower VSG MFI compared to DMSO controls (Fig 5B). Because phenothiazine is such a potent growth inhibitor, we tested whether lower concentrations of the drug might produce the effect on VSG in healthier parasites. We found that a 3d treatment with 16μM phenothiazine produced an effect on VSG MFI but that this was not the case at lower concentrations. We observed almost no effect on *EP1/GFP* transcript levels at these lower concentrations (Fig 5C and S9 Table). In addition, treatment with another growth inhibitor, clemastine fumarate, produced altered VSG MFI with very little effect on *EP1/GFP* expression (Fig 5C). All of the previously reported compounds that increased *EP1* transcript levels and altered VSG MFI also induced growth inhibition [12], so it is difficult to disentangle whether the altered VSG MFI is a non-specific effect in sick parasites or whether it is in some cases a consequence of altered *EP1* transcript levels.

The expression for a number of transcripts associated with differentiation is altered following treatment with spironolactone and eflornithine

Treatment with either eflornithine and spironolactone increased *EP1/GFP* expression in our bloodstream reporter cells, and this made us wonder whether other transcripts associated with differentiation show altered expression levels in drug treated parasites. While phenothiazine also increased *EP1/GFP* expression, we worried that this effect might be a non-specific stress response, and accordingly did not test phenothiazine's effect on other differentiation-related transcripts. We treated parasites with either eflornithine or spironolactone for three days, isolated RNA, and performed qPCR to ask whether expression levels were altered for a subset of genes whose expression changes during differentiation to procyclic forms [52]. In addition to

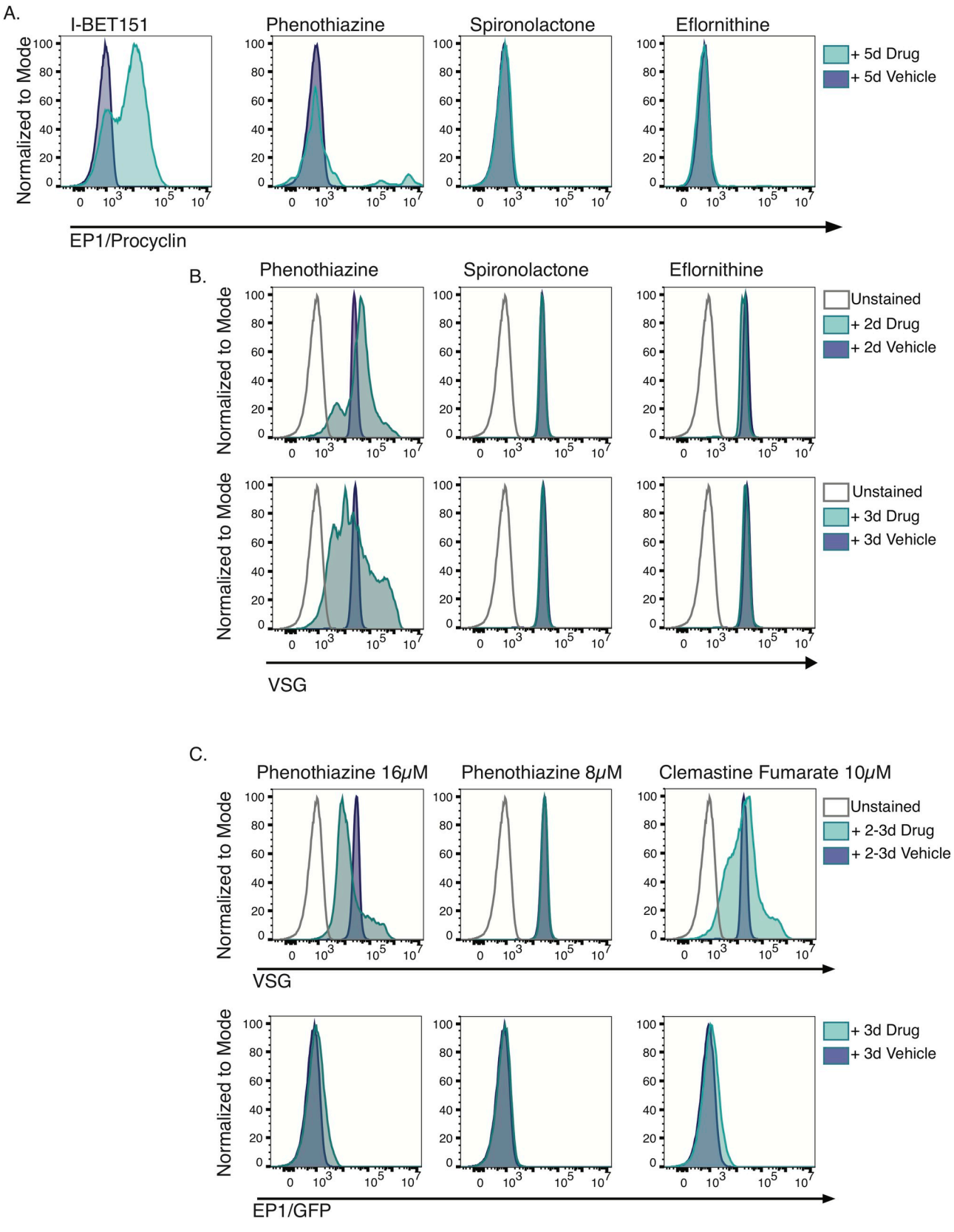
A.
I-BET151
Phenothiazine
Spironolactone
Eflornithine
Normalized to Mode
+ 5d Drug
+ 5d Vehicle
EP1/Procyclin
B.
Phenothiazine
Spironolactone
Eflornithine
Normalized to Mode
Unstained
+ 2d Drug
+ 2d Vehicle
Unstained
+ 3d Drug
+ 3d Vehicle
VSG
C.
Phenothiazine 16μM
Phenothiazine 8μM
Clemastine Fumarate 10μM
Normalized to Mode
Unstained
+ 2-3d Drug
+ 2-3d Vehicle
VSG
+ 3d Drug
+ 3d Vehicle
EP1/GFP

Fig 5. Treatment with phenothiazine, spironolactone and eflornithine does not result in detectable levels of procyclin protein on the cell surface. (A) Flow cytometry plots of bloodstream parasites treated for 5 days with the indicated drug or vehicle control and stained with fluorescent anti-procyclin antibodies. The bromodomain inhibitor I-BET151 was used as a positive control. (B) Flow cytometry plots of bloodstream parasites treated for 3 days with the indicated drug or vehicle control and stained with fluorescent anti-VSG antibodies. C) Flow cytometry plots of bloodstream parasites treated for 3 days (Phenothiazine) or 2 days (Clemastine Fumarate) with the indicated drug or vehicle control and stained with fluorescent anti-VSG antibodies (Top panel). (Bottom panel) *EP1/GFP* expression after treatment with the indicated drugs as in top panel.

https://doi.org/10.1371/journal.pntd.0007790.g005

an increase in *EP1* and *GFP* transcript levels in drug treated cells, we also observed an increase in transcript levels for Procyclic Associated Gene 2 (*PAG2*, *Tb927.10.10220*), which is found just downstream of *EP1* in the same Polycistronic Transcription Unit (PTU) and is known to have increased expression during differentiation (Fig 6). Another surface protein expressed in early procyclic parasites (*GPEET*, *Tb927.6.510*) showed an increase in eflornithine treated parasites, but this increase was not statistically significant. Because differentiating parasites must alter their metabolism to adapt to the insect midgut, we also checked expression levels for a number of genes associated with these changes in metabolism. Both hexokinase (*HK1*, *Tb927.10.2010*) and glycosomal membrane protein (*GIM5B*, *Tb927.9.11600*) show an initial dip in expression levels following initiation of differentiation and then a slow increase in expression, while glycosomal fructose biphosphate aldolase (*ALD*, *Tb927.10.5620*) and pyruvate kinase (*PYK1*, *Tb927.10.14140*) show a monotonic decrease in expression following initiation of differentiation [52]. We observed a subtle but statistically significant decrease in *PYK1*, *GIM5B*, and *HK1* following treatment with eflornithine and a decrease in *HK1* and *ALD* following treatment with spironolactone. No changes were observed in splicing factor 1 (*SF1*, *Tb927.10.9400*), which we used as a negative control as it has not previously been associated with changes in expression for differentiating parasites (Fig 6). It should be emphasized that changes in expression levels for differentiation-associated genes in our drug treated parasites are much lower than those observed when we induced differentiation in our *EP1/GFP* reporter parasites using a three day treatment with 6mM cis-aconitate and incubation at 27˚C (S3A Fig) and for what has been reported in the literature [52]. We note that we did not observe a decrease in transcript levels for either *GIM5B* or *HK1* in our differentiation-induced reporter parasites at 3 days but we did detect this decrease at earlier time points (S3B Fig) This is consistent with the previously reported transient dip in expression levels for these genes observed at early time points prior to 72 hours in the literature [52]. Although the expression changes are muted compared to those in differentiating cells, it is interesting that small changes in *EP1* expression in eflornithine and spironolactone treated parasites are accompanied by other small changes in expression levels for a subset of genes known to be associated with differentiation. We conclude that the effect of both eflornithine and spironolactone is not solely confined to genes associated with changes in the proteins that make up the parasite surface, and may additionally initiate multiple components of the differentiation program.

Discussion

The flow cytometry screen described here allowed us to identify compounds that inhibited trypanosome growth, which can be used as a starting point for alternate trypanosomiasis therapeutics. We purposely used U.S. and foreign approved compounds because their toxicity is better characterized than those of new compounds, which might streamline drug development should promising candidates be found. However, there is no reason that other drug libraries could not be screened using the same methods described here. Our library consisted of ~20 96-well plates, each of which took ~1h to screen. We typically screened 6 plates a day, allowing us to complete a full screen of the 1,585 compounds in duplicate within 2 weeks. While we conducted a medium-throughput screen using 96 well plates, flow cytometry systems can now

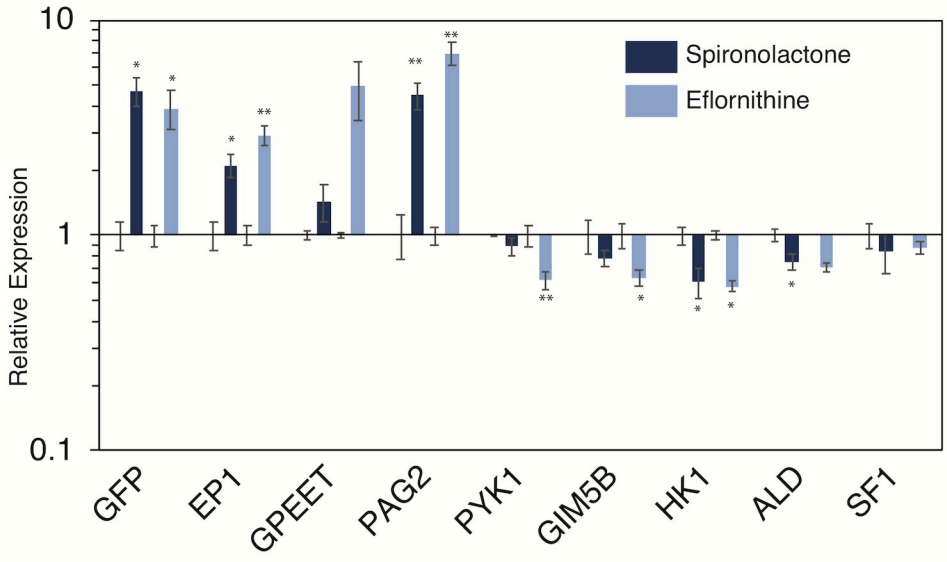

Fig 6. Treatment with spironolactone and eflornithine changes expression levels for a subset of differentiation associated genes. Q-PCR experiment showing relative expression levels for indicated genes in parasites treated for 3 days with 33μM spironolactone, eflornithine, or vehicle control. Error bars indicate standard error of 3 biological replicates. *, **, *** indicates $p < 0.05$, $p < 0.01$, and $p < 0.001$ respectively as measured by an unpaired, two-sided Student's t-test. Note, relative expression is plotted on a log scale.

https://doi.org/10.1371/journal.pntd.0007790.g006

accommodate screening using 1,536 well plates, allowing researchers to screen 50,000 wells per day [53,54]. These technologies would allow for very rapid high-throughput screens.

Our screen uncovered 154 compounds that were slightly to highly inhibitory for trypanosome parasite growth. We were able to confirm a small subset of these by ordering fresh drugs from Sigma-Aldrich and performing growth and IC_{50} assays. 8 of the most highly inhibitory drugs had previously been shown to have effects on *T. brucei* growth, 1 had previously been shown to affect growth in *T. evansi*, and 10 had been shown to inhibit growth in *T. cruzi*. To our knowledge, the remaining 16 compounds that were in the highest category for growth inhibition have not previously been reported to affect *T. brucei* growth. We hope that our toxicity data in conjunction with already existing toxicity data can help to prioritize which of these drugs might be most promising as novel therapeutics. It is worth noting that pentamidine, a trypanosomiasis drug currently in active use, was sorted into the moderately inhibitory category, implying that the 102 compounds in this category could have potential as trypanosomiasis therapeutics.

We were able to confirm the growth inhibitory effects of a small subset of drugs across the inhibitory categories by ordering fresh drugs from Sigma-Aldrich and performing growth and IC_{50} assays. One of the compounds we tested (triprolidine) was a false positive, for which we don't have a good explanation. It is possible that evaporation of the drug plate resulted in some compounds being tested at higher than the intended concentrations, which would be consistent with the fact that we did find growth inhibitory effects of triprolidine at high concentrations in the IC_{50} assay. That said, we were able to confirm that the majority of compounds we tested had growth inhibitory effects consistent with the drug screen data. It is also worth noting that our screen likely contained some false negatives. Among other reasons, the hygromycin resistance marker used to select for the *EP1/GFP* reporter cells may have inactivated some of the drugs in the library due to phosphorylation.

We also showed proof of concept for a reporter strain that can be used to track the molecular events that initiate surface remodeling during trypanosome differentiation from the bloodstream form to the procyclic form, an event that is critical to life cycle progression. We first showed that expression of *EP1/GFP* in our reporter line behaves as expected in bloodstream, procyclic and differentiating cells. One weakness of our reporter is that it was used in a monomorph strain rather than a pleomorph strain. While pleomorphs can be treated *in vitro* to closely mimic developmental transitions from bloodstream to procyclic parasites via the intermediate stumpy stage that is observed in the wild, monomorph lines are incapable of stumpy formation, making them a less physiological model. With this in mind, we created a pleomorphic *EP1/GFP* reporter strain and piloted it for use in flow cytometric screens. Unfortunately, *EP1/GFP* expression in these pleomorphic lines is much more variable than in the monomorph lines, and tends to increase with increasing parasite density (S10 Table and S4 Fig), which is consistent with preadaptation of stumpy parasites for transition to the insect vector [47]. Therefore, we decided to use monomorph lines for screening purposes, and for any drugs that produced procyclin protein on the surface, these drugs could be separately tested in pleomorph lines using anti-procyclin antibodies. Monomorph lines have been successfully used by others to identify factors important for differentiation when coupled with follow-up studies in pleomorph parasites [55–57].

This study demonstrates that our developmental reporter line can be used to conduct flow-cytometry based small molecule drug screens. Importantly, our screening pipeline was developed such that growth inhibition can be tracked at the same time as the transcript abundance for our gene of interest. This allowed us to quickly identify drugs that might cause a non-specific increase in *EP1/GFP* expression, perhaps due to a stress response induced by the drug. Phenothiazine's effect on *EP1/GFP* transcript levels may well be non-specific, as the drug is a potent growth inhibitor, although many other drugs that inhibited growth did not have this effect. Our screen is similar in concept to a previously reported screen that tracked *EP1* expression levels using a GUS reporter system [11,12]. This reporter was also used in a medium-throughput screen of 7,500 compounds in a 96 well plate format using drug concentrations between 1 and 20μg/ml. For comparison, our screening concentration of 33μM corresponds to a 6–13μg/ml treatment for our *EP1/GFP* hits. *GFP* expression was found to be ~26 times higher when we treated parasites with cis-aconitate than when we treated them with eflornithine (Fig 6 and S3 Fig). This phenomenon was also observed in the GUS screen; compound-induced GUS signals were up to 5000-fold lower than when parasites were treated with cis-aconitate [12]. All of the hits from the GUS screen were shown to inhibit parasite growth, and the top hits also had an effect on surface VSG MFI [12]. Similar to the hits from the previous study, phenothiazine-treated parasites showed inhibited growth, higher transcript levels of *EP1*, and altered VSG MFI (Fig 5B and 5C). However, while *EP1* transcript levels were higher in eflornithine and spironolactone-treated parasites, neither of these compounds showed effects on parasite growth or VSG MFI. To our knowledge, the level of procyclin protein expressed on the parasite surface was not tested in parasites treated with compounds that induced higher GUS signals in the previous study. In our study, we failed to identify any compounds that produced procyclin protein on the surface of parasites, underscoring the already established paradigm that additional developmental steps may be required to remodel the parasite surface following transcription of the relevant RNAs. In addition, defects in glycosylation of the procyclin protein and/or defects in the addition of the GPI anchor could also explain the lack of procyclin protein observed on the surface of the parasites [65–68]. Given that the bromodomain inhibitor I-BET151 has previously been shown to increase both RNA and protein levels of procyclin [10], a more targeted screen using a library of epigenetic inhibitors might uncover more compounds that lead to this phenotype in the *EP1/GFP* reporter line.

While the GUS reporter system has been put to excellent use to identify compounds that increase transcript levels of *EP1*, a fluorescence-based reporter might have some advantages when performing genetic screens for native factors that are important for this process during developmental transitions. For example, parasites could be transfected with either an RNAi library or an overexpression library in bulk, and fluorescence positive parasites could be physically separated from the population using fluorescence activated cell sorting. This would allow for easy identification of gene products that increase the transcription and/or stability of procyclin, which could provide insights into molecular mechanisms for surface remodeling that occurs during developmental transitions.

Treatment with both spironolactone and eflornithine did not affect expression of *EP1* alone, as we found effects on several other differentiation-associated genes. This phenotype was also previously observed for I-BET151, although its effects on differentiation associated genes were of greater magnitude [10]. In future, it would be interesting to test whether artificially increasing *EP1* levels via overexpression of the gene is sufficient to induce expression changes in other differentiation-associated genes. It should be noted that we have no data to support a direct effect for these compounds on *EP1/GFP* expression, and the changes in transcript abundance for both *EP1* and the other differentiation-associated genes tested may well be due to secondary effects.

While eflornithine had previously been reported to induce a stumpy-like, but developmentally incompetent, transition in monomorphic cells [46], the effect of spironolactone on *T. brucei* physiology has not been studied. In mammalian systems, spironolactone is an anti-androgen drug that non-selectively antagonizes mineralcorticoid receptors, including both progesterone and androgen receptors. It is used as a hypertensive agent to decrease morbidity and mortality of heart failure [58]. To our knowledge, no proteins with similarity to mineralocorticoid receptors have been identified in *T. brucei*. We used BLAST to interrogate various kinetoplastid genomes with both the DNA-binding domain of the human glucocorticoid receptor and the ligand-binding domain of the mineralocorticoid receptor. While no hits were uncovered in *T. brucei*, we did obtain a few hits for genes in *T. cruzi* and *Leishmania panamensis* using the DNA-binding domain. All of the identified genes in *T. cruzi* (Tc00.1047053504039.110, Tc00.1047053506769.55, and Tc00.1047053510555.21) with an E value of less than 0.01 were for hypothetical proteins and ranged from 26%-33% identities. All three of them were also shown to be transcriptionally downregulated after infection in amastigotes and upregulated in epimastigotes [59]. For BLAST with the ligand-binding domain of the mineralocorticoid receptor, we only obtained two hits with an E value of less than 0.05, one in *Perkinsela* (XU18_4875) and the other in *Leishmania Mexicana* (LMXM_29_2680). Both genes code for hypothetical proteins and had a 33–34% identity with the query. Future studies could potentially uncover the target of spironolactone in *T. brucei* by overexpressing a library of *T. brucei* ORFs and assaying for a decrease in *GFP* expression in spironolactone treated *EP1/GFP* reporter cells. These types of overexpression suppressor screens have previously been used successfully to identify drug targets in yeast and other organisms [60]. With the gene target identified, genetic studies could uncover the role of this target (if any) in the initiation of transcription or stabilization of *EP1* transcript following the appropriate developmental signals in bloodstream form cells.

While we focused on generating alternate trypanosomiasis therapeutics by inducing life cycle progression in *T. brucei*, this strategy could likewise be applied to other causative agents for neglected disease. Indeed, this strategy is actively being pursued for treatment of malaria, toxoplasmosis, and schistosomiasis [61–63]. We think our reporter strain (and other developmental reporter strains such as the Pad1-GFP strain that tracks stumpy formation [64]) offer a powerful tool to perform genetic screens for developmental phenotypes. With the increasing availability of knockdown and overexpression libraries in *T. brucei*, there is great potential to

uncover new life cycle-specific biological roles for the numerous proteins in *T. brucei* that are annotated as hypothetical. The combination of fluorescent reporter strains with high-throughput flow cytometry assays facilitates screening strategies that are both less labor-intensive and time-intensive than previous methods.

Supporting information

S1 Fig. Triprolidine does not affect *T. brucei* growth at low concentrations. Percent growth inhibition over a range of concentrations for the indicated drug. Data were fitted and indicated values calculated using the GRMetrics R package. GR_{50}, the concentration at which the effect reaches a growth rate (GR) value of 0.5 based on interpolation of the fitted curve (dashed lines). GIC_{50}, the drug concentration at half-maximal effect for calculated growth rate. r^2 GR, the coefficient of determination for how well the GR curve fits to the data points. IC_{50}, the concentration at which relative cell count = 0.5. r^2 IC_{50}, the coefficient of determination for how well the traditional curve fits to the data points.
(TIF)

S2 Fig. A) Anti-procyclin western blot for parasites isolated after 3d of treatment with the indicated drug. Procyclic parasites were used as a positive control. Anti-H3 was used as a loading control. Note that the samples ran high toward the right-hand side of the blot. B) Anti-procyclin western blot for parasites isolated after 2d or 3d of treatment with the indicated drug. Procyclic parasites were used as a positive control. Anti-H3 was used as a loading control. Because phenothiazine-treated parasites were so sick it was difficult to get sufficient numbers of cells for the assay; consequently, these samples and their controls are loaded with less protein.
(TIF)

S3 Fig. A) Gene expression for genes associated with differentiation in bloodstream parasites treated with 6mM cis-aconitate and incubated at 27˚C for 3 days. B) Gene expression of *HK1* and *GIM5B* for parasites isolated after 1 or 2 days induction of differentiation, as in A.
(TIF)

S4 Fig. *EP1/GFP* expression for Antat 1.1 *EP1/GFP* reporter parasites seeded at 1/10 the indicated density and analyzed after 1 day of growth.
(TIF)

S1 Table. Information on the drugs identified as most highly inhibitory for *T. brucei* growth.
(XLSX)

S2 Table. Drugs identified as most highly inhibitory for *T. brucei* growth.
(XLSX)

S3 Table. Drugs identified as inhibitory for *T. brucei* growth.
(XLSX)

S4 Table. Drugs identified as slightly inhibitory for *T. brucei* growth.
(XLSX)

S5 Table. Pubchem toxicity info on drugs identified as inhibitory for *T. brucei* growth.
(XLSX)

S6 Table. Toxicity values for drugs verified to inhibit *T. brucei* growth.
(XLSX)

S7 Table. Drugs that increase expression of *EP1/GFP*.
(XLSX)

S8 Table. Number of live cells following growth at 33μM triprolidine.
(XLSX)

S9 Table. *EP1/GFP* and *VSG* expression at low concentrations of phenothiazine.
(XLSX)

S10 Table. *EP1/GFP* expression for Antat 1.1 *EP1/GFP* reporter parasites seeded at 1/10 the indicated density and analyzed after 1 day of growth.
(XLSX)

Acknowledgments

We thank the members of the Harvey Mudd College Department of Biology for helpful discussions. We thank Gracyn Buenconsejo and Lucy Paddock for research assistance. We also thank Monica Mugnier for helpful comments on the manuscript and Christian Janzen for the anti-H3 antibody.

Author Contributions

Conceptualization: Madison Elle Walsh, Danae Schulz.

Data curation: Madison Elle Walsh, Danae Schulz.

Formal analysis: Madison Elle Walsh, Danae Schulz.

Investigation: Madison Elle Walsh, Eleanor Mary Naudzius, Savanah Jessica Diaz, Theodore William Wismar.

Methodology: Madison Elle Walsh, Danae Schulz.

Project administration: Danae Schulz.

Resources: Mikhail Martchenko Shilman, Danae Schulz.

Software: Madison Elle Walsh, Danae Schulz.

Supervision: Danae Schulz.

Validation: Danae Schulz.

Visualization: Madison Elle Walsh, Danae Schulz.

Writing – original draft: Madison Elle Walsh, Danae Schulz.

Writing – review & editing: Mikhail Martchenko Shilman, Danae Schulz.

References

1. Bukachi SA, Wandibba S, Nyamongo IK. The socio-economic burden of human African trypanosomiasis and the coping strategies of households in the South Western Kenya foci. PLoS Negl Trop Dis. 2017 Oct 1; 11(10):e0006002. https://doi.org/10.1371/journal.pntd.0006002 PMID: 29073144
2. Barrett MP, Vincent IM, Burchmore RJS, Kazibwe AJN, Matovu E. Drug resistance in human African trypanosomiasis. Future Microbiol. 2011 Sep 1; 6(9):1037–47. https://doi.org/10.2217/fmb.11.88 PMID: 21958143
3. Stijlemans B, Caljon G, Van Den Abbeele J, Van Ginderachter JA, Magez S, De Trez C. Immune Evasion Strategies of Trypanosoma brucei within the Mammalian Host: Progression to Pathogenicity. Front Immunol. 2016 Jan 1; 7:233. https://doi.org/10.3389/fimmu.2016.00233 PMID: 27446070

4. Cross GAM, Kim H-S, Wickstead B. Capturing the variant surface glycoprotein repertoire (the VSGnome) of Trypanosoma brucei Lister 427. Molecular & Biochemical Parasitology. 2014 Jun 1; 195 (1):59–73.
5. Smith TK, Bringaud F, Nolan DP, Figueiredo LM. Metabolic reprogramming during the Trypanosoma brucei life cycle. F1000Res [Internet]. 2017 Jan 1; 6. Available from: http://eutils.ncbi.nlm.nih.gov/entrez/eutils/elink.fcgi?dbfrom=pubmed&id=28620452&retmode=ref&cmd=prlinks
6. Jensen BC, Sivam D, Kifer CT, Myler PJ, Parsons M. Widespread variation in transcript abundance within and across developmental stages of Trypanosoma brucei. BMC Genomics. 2009 Jan 1; 10 (1):482.
7. Kabani S, Fenn K, Ross A, Ivens A, Smith TK, Ghazal P, et al. Genome-wide expression profiling of in vivo-derived bloodstream parasite stages and dynamic analysis of mRNA alterations during synchronous differentiation in Trypanosoma brucei. BMC Genomics. 2009 Jan 1; 10(1):427.
8. Nilsson D, Gunasekera K, Mani J, Osteras M, Farinelli L, Baerlocher L, et al. Spliced Leader Trapping Reveals Widespread Alternative Splicing Patterns in the Highly Dynamic Transcriptome of Trypanosoma brucei. Parsons M, editor. PLoS Pathog. 2010 Aug 5; 6(8):e1001037. https://doi.org/10.1371/journal.ppat.1001037 PMID: 20700444
9. Vassella E, Acosta-Serrano A, Studer E, Lee SH, Englund PT, Roditi I. Multiple procyclin isoforms are expressed differentially during the development of insect forms of Trypanosoma brucei. J Mol Biol. 2001 Sep 28; 312(4):597–607. https://doi.org/10.1006/jmbi.2001.5004 PMID: 11575917
10. Schulz D, Mugnier MR, Paulsen E-M, Kim H-S, Chung CW, Tough DF, et al. Bromodomain Proteins Contribute to Maintenance of Bloodstream Form Stage Identity in the African Trypanosome. Carruthers VB, editor. PLoS Biol. 2015 Dec 8; 13(12):e1002316–38. https://doi.org/10.1371/journal.pbio.1002316 PMID: 26646171
11. Sbicego S, Vassella E, Kurath U, Blum B, Roditi I. The use of transgenic Trypanosoma brucei to identify compounds inducing the differentiation of bloodstream forms to procyclic forms. Molecular & Biochemical Parasitology. 1999 Nov 30; 104(2):311–22.
12. Wenzler T, Schumann Burkard G, Schmidt RS, Mäser P, Bergner A, Roditi I, et al. A new approach to chemotherapy: drug-induced differentiation kills African trypanosomes. Sci Rep. 2016 Jan 1; 6:22451. https://doi.org/10.1038/srep22451 PMID: 26931380
13. McDonald L, Cayla M, Ivens A, Mony BM, MacGregor P, Silvester E, et al. Non-linear hierarchy of the quorum sensing signalling pathway in bloodstream form African trypanosomes. PLoS Pathog. 2018; 14 (6):e1007145. https://doi.org/10.1371/journal.ppat.1007145 PMID: 29940034
14. Rico E, Ivens A, Glover L, Horn D, Matthews KR. Genome-wide RNAi selection identifies a regulator of transmission stage-enriched gene families and cell-type differentiation in Trypanosoma brucei. PLoS Pathog. 2017 Mar 1; 13(3):e1006279. https://doi.org/10.1371/journal.ppat.1006279 PMID: 28334017
15. Rojas F, Silvester E, Young J, Milne R, Tettey M, Houston DR, et al. Oligopeptide Signaling through TbGPR89 Drives Trypanosome Quorum Sensing. Cell. 2019 Jan 10; 176(1–2):306–317.e16. https://doi.org/10.1016/j.cell.2018.10.041 PMID: 30503212
16. Mugo E, Clayton C. Expression of the RNA-binding protein RBP10 promotes the bloodstream-form differentiation state in Trypanosoma brucei. PLoS Pathog. 2017 Aug 1; 13(8):e1006560. https://doi.org/10.1371/journal.ppat.1006560 PMID: 28800584
17. Jha BA, Gazestani VH, Yip CW, Salavati R. The DRBD13 RNA binding protein is involved in the insect-stage differentiation process of Trypanosoma brucei. FEBS Lett. 2015 Jul 8; 589(15):1966–74. https://doi.org/10.1016/j.febslet.2015.05.036 PMID: 26028502
18. Kolev NG, Ramey-Butler K, Cross GAM, Ullu E, Tschudi C. Developmental Progression to Infectivity in Trypanosoma brucei Triggered by an RNA-Binding Protein. Science. 2012 Dec 6; 338(6112):1352–3. https://doi.org/10.1126/science.1229641 PMID: 23224556
19. Walrad P, Paterou A, Acosta-Serrano A, Matthews KR. Differential Trypanosome Surface Coat Regulation by a CCCH Protein That Co-Associates with procyclin mRNA cis-Elements. Ullu E, editor. PLoS Pathog. 2009 Feb 27; 5(2):e1000317. https://doi.org/10.1371/journal.ppat.1000317 PMID: 19247446
20. Hertz-Fowler C, Figueiredo LM, Quail MA, Becker M, Jackson A, Bason N, et al. Telomeric Expression Sites Are Highly Conserved in Trypanosoma brucei. Hall N, editor. PLoS ONE. 2008 Oct 27; 3(10): e3527. https://doi.org/10.1371/journal.pone.0003527 PMID: 18953401
21. Ziegelbauer K, Quinten M, Schwarz H, Pearson TW, Overath P. Synchronous differentiation of Trypanosoma brucei from bloodstream to procyclic forms in vitro. Eur J Biochem. 1990 Sep 11; 192(2):373–8. https://doi.org/10.1111/j.1432-1033.1990.tb19237.x PMID: 1698624
22. Hafner M, Niepel M, Chung M, Sorger PK. Growth rate inhibition metrics correct for confounders in measuring sensitivity to cancer drugs. Nature Methods. 2016 Jun; 13(6):521–7. https://doi.org/10.1038/nmeth.3853 PMID: 27135972

23. Lu Q, Wei W, Kowalski PE, Chang ACY, Cohen SN. EST-based genome-wide gene inactivation identifies ARAP3 as a host protein affecting cellular susceptibility to anthrax toxin. Proc Natl Acad Sci USA. 2004 Dec 7; 101(49):17246–51. https://doi.org/10.1073/pnas.0407794101 PMID: 15569923

24. Zilbermintz L, Leonardi W, Tran SH, Zozaya J, Mathew-Joseph A, Liem S, et al. Cross-inhibition of pathogenic agents and the host proteins they exploit. Scientific Reports [Internet]. 2016 Dec [cited 2019 Dec 1]; 6(1). Available from: http://www.nature.com/articles/srep34846

25. Boda C, Enanga B, Courtioux B, Breton J-C, Bouteille B. Trypanocidal activity of methylene blue. Evidence for in vitro efficacy and in vivo failure. Chemotherapy. 2006; 52(1):16–9. https://doi.org/10.1159/000090236 PMID: 16340192

26. Cross GA, Klein RA, Linstead DJ. Utilization of amino acids by Trypanosoma brucei in culture: L-threonine as a precursor for acetate. Parasitology. 1975 Oct; 71(2):311–26. https://doi.org/10.1017/s0031182000046758 PMID: 1187188

27. Gutiérrez-Correa J, Krauth-Siegel RL, Stoppani AOM. Phenothiazine radicals inactivate Trypanosoma cruzi dihydrolipoamide dehydrogenase: enzyme protection by radical scavengers. Free Radic Res. 2003 Mar; 37(3):281–91. https://doi.org/10.1080/1071576021000046622 PMID: 12688423

28. Kölzer M, Weitzel K, Göringer HU, Thines E, Opatz T. Synthesis of bioactive 2-aza-analogues of ipecac and alangium alkaloids. ChemMedChem. 2010 Sep 3; 5(9):1456–64. https://doi.org/10.1002/cmdc.201000230 PMID: 20575140

29. Rosenkranz V, Wink M. Alkaloids induce programmed cell death in bloodstream forms of trypanosomes (Trypanosoma b. brucei). Molecules. 2008 Oct 3; 13(10):2462–73. https://doi.org/10.3390/molecules13102462 PMID: 18833031

30. Benaim BG, Garcia CRS. Targeting calcium homeostasis as the therapy of Chagas' disease and leishmaniasis—a review. Trop Biomed. 2011 Dec; 28(3):471–81. PMID: 22433874

31. De Rycker M, Thomas J, Riley J, Brough SJ, Miles TJ, Gray DW. Identification of Trypanocidal Activity for Known Clinical Compounds Using a New Trypanosoma cruzi Hit-Discovery Screening Cascade. PLoS Negl Trop Dis. 2016 Apr; 10(4):e0004584. https://doi.org/10.1371/journal.pntd.0004584 PMID: 27082760

32. Franke De Cazzulo BM, Bernacchi A, Esteva MI, Ruiz AM, Castro JA, Cazzulo JJ. Trypanocidal effect of SKF525A, proadifen, on different developmental forms of Trypanosoma cruzi. Medicina (B Aires). 1998; 58(4):415–8.

33. Hammond DJ, Hogg J, Gutteridge WE. Trypanosoma cruzi: possible control of parasite transmission by blood transfusion using amphiphilic cationic drugs. Exp Parasitol. 1985 Aug; 60(1):32–42. https://doi.org/10.1016/s0014-4894(85)80020-5 PMID: 3926530

34. Kinnamon KE, Poon BT, Hanson WL, Waits VB. In pursuit of drugs for American trypanosomiasis: evaluation of some "standards" in a mouse model. Proc Soc Exp Biol Med. 1997 Dec; 216(3):424–8. https://doi.org/10.3181/00379727-216-44192 PMID: 9402149

35. Morello A, Lipchenca I, Cassels BK, Speisky H, Aldunate J, Repetto Y. Trypanocidal effect of boldine and related alkaloids upon several strains of Trypanosoma cruzi. Comp Biochem Physiol Pharmacol Toxicol Endocrinol. 1994 Mar; 107(3):367–71. https://doi.org/10.1016/1367-8280(94)90063-9 PMID: 8061943

36. Planer JD, Hulverson MA, Arif JA, Ranade RM, Don R, Buckner FS. Synergy testing of FDA-approved drugs identifies potent drug combinations against Trypanosoma cruzi. PLoS Negl Trop Dis. 2014 Jul; 8(7):e2977. https://doi.org/10.1371/journal.pntd.0002977 PMID: 25033456

37. Reimão JQ, Colombo FA, Pereira-Chioccola VL, Tempone AG. In vitro and experimental therapeutic studies of the calcium channel blocker bepridil: detection of viable Leishmania (L.) chagasi by real-time PCR. Exp Parasitol. 2011 Jun; 128(2):111–5. https://doi.org/10.1016/j.exppara.2011.02.021 PMID: 21354141

38. Silva FT, Franco CH, Favaro DC, Freitas-Junior LH, Moraes CB, Ferreira EI. Design, synthesis and antitrypanosomal activity of some nitrofurazone 1,2,4-triazolic bioisosteric analogues. Eur J Med Chem. 2016 Oct 4; 121:553–60. https://doi.org/10.1016/j.ejmech.2016.04.065 PMID: 27318979

39. Anene BM, Ross CA, Anika SM, Chukwu CC. Trypanocidal resistance in Trypanosoma evansi in vitro: effects of verapamil, cyproheptidine, desipramine and chlorpromazine alone and in combination with trypanocides. Vet Parasitol. 1996 Mar; 62(1–2):43–50. https://doi.org/10.1016/0304-4017(95)00856-x PMID: 8638392

40. Dolan RB, Okech G, Alushula H, Mutugi M, Stevenson P, Sayer PD, et al. Homidium bromide as a chemoprophylactic for cattle trypanosomiasis in Kenya. Acta Trop. 1990 Mar; 47(3):137–44. https://doi.org/10.1016/0001-706x(90)90019-v PMID: 1971490

41. Bouteille B, Buguet A. The detection and treatment of human African trypanosomiasis. Res Rep Trop Med. 2012; 3:35–45. https://doi.org/10.2147/RRTM.S24751 PMID: 30890865

42. Chung MC, Gonçalves MF, Colli W, Ferreira EI, Miranda MT. Synthesis and in vitro evaluation of potential antichagasic dipeptide prodrugs of primaquine. J Pharm Sci. 1997 Oct; 86(10):1127–31. https://doi.org/10.1021/js970006v PMID: 9344169

43. Sbaraglini ML, Bellera CL, Fraccaroli L, Larocca L, Carrillo C, Talevi A, et al. Novel cruzipain inhibitors for the chemotherapy of chronic Chagas disease. Int J Antimicrob Agents. 2016 Jul; 48(1):91–5. https://doi.org/10.1016/j.ijantimicag.2016.02.018 PMID: 27216381

44. Chan C, Yin H, Garforth J, McKie JH, Jaouhari R, Speers P, et al. Phenothiazine inhibitors of trypanothione reductase as potential antitrypanosomal and antileishmanial drugs. J Med Chem. 1998 Jan 15; 41(2):148–56. https://doi.org/10.1021/jm960814j PMID: 9457238

45. Seebeck T, Gehr P. Trypanocidal action of neuroleptic phenothiazines in Trypanosoma brucei. Mol Biochem Parasitol. 1983 Nov; 9(3):197–208. https://doi.org/10.1016/0166-6851(83)90097-x PMID: 6144043

46. Giffin BF, McCann PP, Bitonti AJ, Bacchi CJ. Polyamine depletion following exposure to DL-alpha-difluoromethylornithine both in vivo and in vitro initiates morphological alterations and mitochondrial activation in a monomorphic strain of Trypanosoma brucei brucei. J Protozool. 1986 May; 33(2):238–43. https://doi.org/10.1111/j.1550-7408.1986.tb05599.x PMID: 3090240

47. Rico E, Rojas F, Mony BM, Szöőr B, MacGregor P, Matthews KR. Bloodstream form pre-adaptation to the tsetse fly in Trypanosoma brucei. Front Cell Infect Microbiol. 2013 Jan 1; 3:78. https://doi.org/10.3389/fcimb.2013.00078 PMID: 24294594

48. Ramires FJA, Salemi VMC, Ianni BM, Fernandes F, Martins DG, Billate A, et al. Aldosterone antagonism in an inflammatory state: evidence for myocardial protection. J Renin Angiotensin Aldosterone Syst. 2006 Sep; 7(3):162–7. https://doi.org/10.3317/jraas.2006.026 PMID: 17094053

49. Kumar A, Naguib YW, Shi Y, Cui Z. A method to improve the efficacy of topical eflornithine hydrochloride cream. Drug Deliv. 2016 Jun; 23(5):1495–501. https://doi.org/10.3109/10717544.2014.951746 PMID: 25182303

50. Marcu A, Schurigt U, Müller K, Moll H, Krauth-Siegel RL, Prinz H. Inhibitory effect of phenothiazine- and phenoxazine-derived chloroacetamides on Leishmania major growth and Trypanosoma brucei trypanothione reductase. Eur J Med Chem. 2016 Jan 27; 108:436–43. https://doi.org/10.1016/j.ejmech.2015.11.023 PMID: 26708110

51. Kim H-S, Park SH, Günzl A, Cross GAM. MCM-BP Is Required for Repression of Life-Cycle Specific Genes Transcribed by RNA Polymerase I in the Mammalian Infectious Form of Trypanosoma brucei. Louis EJ, editor. PLoS ONE. 2013 Feb 25; 8(2):e57001. https://doi.org/10.1371/journal.pone.0057001 PMID: 23451133

52. Queiroz R, Benz C, Fellenberg K, Hoheisel JD, Clayton C. Transcriptome analysis of differentiating trypanosomes reveals the existence of multiple post-transcriptional regulons. BMC Genomics. 2009 Jan 1; 10(1):495.

53. Ding M, Kaspersson K, Murray D, Bardelle C. High-throughput flow cytometry for drug discovery: principles, applications, and case studies. Drug Discovery Today. 2017 Dec; 22(12):1844–50. https://doi.org/10.1016/j.drudis.2017.09.005 PMID: 28916303

54. Joslin J, Gilligan J, Anderson P, Garcia C, Sharif O, Hampton J, et al. A Fully Automated High-Throughput Flow Cytometry Screening System Enabling Phenotypic Drug Discovery. SLAS DISCOVERY: Advancing Life Sciences R&D. 2018 Aug; 23(7):697–707.

55. Jones NG, Thomas EB, Brown E, Dickens NJ, Hammarton TC, Mottram JC. Regulators of Trypanosoma brucei Cell Cycle Progression and Differentiation Identified Using a Kinome-Wide RNAi Screen. Horn D, editor. PLoS Pathogens. 2014 Jan 16; 10(1):e1003886. https://doi.org/10.1371/journal.ppat.1003886 PMID: 24453978

56. Mony BM, MacGregor P, Ivens A, Rojas F, Cowton A, Young J, et al. Genome-wide dissection of the quorum sensing signalling pathway in Trypanosoma brucei. Nature. 2014 Jan 30; 505(7485):681–5. https://doi.org/10.1038/nature12864 PMID: 24336212

57. Rico E, Ivens A, Glover L, Horn D, Matthews KR. Genome-wide RNAi selection identifies a regulator of transmission stage-enriched gene families and cell-type differentiation in Trypanosoma brucei. PLoS Pathog. 2017; 13(3):e1006279. https://doi.org/10.1371/journal.ppat.1006279 PMID: 28334017

58. Sica DA. Pharmacokinetics and pharmacodynamics of mineralocorticoid blocking agents and their effects on potassium homeostasis. Heart Fail Rev. 2005 Jan; 10(1):23–9. https://doi.org/10.1007/s10741-005-2345-1 PMID: 15947888

59. Li Y, Shah-Simpson S, Okrah K, Belew AT, Choi J, Caradonna KL, et al. Transcriptome Remodeling in Trypanosoma cruzi and Human Cells during Intracellular Infection. PLoS Pathog. 2016 Apr; 12(4):e1005511. https://doi.org/10.1371/journal.ppat.1005511 PMID: 27046031

60. Prelich G. Gene overexpression: uses, mechanisms, and interpretation. Genetics. 2012 Mar; 190(3):841–54. https://doi.org/10.1534/genetics.111.136911 PMID: 22419077

61. Bougdour A, Maubon D, Baldacci P, Ortet P, Bastien O, Bouillon A, et al. Drug inhibition of HDAC3 and epigenetic control of differentiation in Apicomplexa parasites. J Exp Med. 2009 Apr 13; 206(4):953–66. https://doi.org/10.1084/jem.20082826 PMID: 19349466

62. Chua MJ, Robaa D, Skinner-Adams TS, Sippl W, Andrews KT. Activity of bromodomain protein inhibitors/binders against asexual-stage Plasmodium falciparum parasites. Int J Parasitol Drugs Drug Resist. 2018; 8(2):189–93. https://doi.org/10.1016/j.ijpddr.2018.03.001 PMID: 29631126

63. Padalino G, Ferla S, Brancale A, Chalmers IW, Hoffmann KF. Combining bioinformatics, cheminformatics, functional genomics and whole organism approaches for identifying epigenetic drug targets in Schistosoma mansoni. Int J Parasitol Drugs Drug Resist. 2018; 8(3):559–70. https://doi.org/10.1016/j.ijpddr.2018.10.005 PMID: 30455056

64. Batram C, Jones NG, Janzen CJ, Markert SM, Engstler M. Expression site attenuation mechanistically links antigenic variation and development in Trypanosoma brucei. eLife. 2014 Jan 1; 3:e02324. https://doi.org/10.7554/eLife.02324 PMID: 24844706

65. Güther MLS, Beattie K, Lamont DJ, James J, Prescott AR, Ferguson MAJ. Fate of Glycosylphosphatidylinositol (GPI)-Less Procyclin and Characterization of Sialylated Non-GPI-Anchored Surface Coat Molecules of Procyclic-Form *Trypanosoma brucei*. Eukaryotic Cell. 2009 Sep; 8(9):1407–17. https://doi.org/10.1128/EC.00178-09 PMID: 19633269

66. Treumann A, Zitzmann N, Hülsmeier A, Prescott AR, Almond A, Sheehan J, et al. Structural characterisation of two forms of procyclic acidic repetitive protein expressed by procyclic forms of Trypanosoma brucei. J Mol Biol. 1997 Jun 20; 269(4):529–47. https://doi.org/10.1006/jmbi.1997.1066 PMID: 9217258

67. Lillico S, Field MC, Blundell P, Coombs GH, Mottram JC. Essential Roles for GPI-anchored Proteins in African Trypanosomes Revealed Using Mutants Deficient in GPI8. Gilmore R, editor. Molecular Biology of the Cell. 2003 Mar; 14(3):1182–94. https://doi.org/10.1091/mbc.E02-03-0167 PMID: 12631733

68. Acosta-Serrano A, Cole RN, Mehlert A, Lee MG, Ferguson MA, Englund PT. The procyclin repertoire of Trypanosoma brucei. Identification and structural characterization of the Glu-Pro-rich polypeptides. J Biol Chem. 1999 Oct 15; 274(42):29763–71. https://doi.org/10.1074/jbc.274.42.29763 PMID: 10514452